Global Sensitivity Analysis of an Energy Harvesting System with Periodic Excitation via Sobol' Indices

Estevão Fuzaro de Almeida[1a], Lucas Veronez Goulart Ferreira [1b], Estênio Fuzaro de Almeida[1c], João Pedro Fernandes Salvador[1d]

[1]São Paulo State University (FEIS-UNESP) - Ilha Solteira, SP, Brazil
[a]`estevao.fuzaro@unesp.br`, [b]`lucas.goulart@unesp.br`,
[c]`estenio.fuzaro@unesp.br`, [d]`jp.salvador@unesp.br`

Abstract Energy harvester performance is directly related to its intrinsic parameters, even small perturbations on these parameters can change significantly the vibrational behavior of the system. This work seeks to determine the most essential parameters in the dynamics of a multimodal energy harvester system with piezoelectric coupling considering the variability of the excitation parameters: force amplitude and angular frequency. An orthogonal decomposition in terms of conditional variances was used to conduct a global sensitivity analysis based on the Sobol' indices to assess the reliance of the collected power on the harvester parameters. This technique is used to determine the variance of each individual and combined parameter in comparison to the total variation of the model. Our results suggests that the angular frequency of the periodical force, which is of an external influence, should be taken into consideration when designing the components of an energy harvester.

Keywords Energy Harvesting, Global Sensitivity Analysis, Sobol' Indices, Polynomial Chaos Expansion

1 Motivation

The design of electrically self-sustaining systems has been an engineering challenge since the creation of electronic devices. Smaller, practical and ecological devices which are independent from batteries could come to light from the solution of this problem and it also creates new possibilities that were previously inconceivable (da Costa Ferreira, 2015).

In this sense, the environmental energy collectors appear as a solution to this problem. These devices capture energy from any source (heat, wind, vibration, etc.) and convert it into electrical energy (Massone A. C. C., 2019). In this way, they are able to supply and sustain the operation of low power equipment, assisting in the design and installation of sensors, transmitters and actuators.

Thus, real systems equipment require a other level of complexity, uncertainty. Treating an energy collector as deterministic disregards its probabilistic variables such as its properties and geometry, which exists due to the manufacturing process and applied quality control, in addition to the external operating conditions of the instrument (Norenberg et al., 2021a).

For a accurate prediction and high fidelity system, the global sensitivity analysis via Sobol' indices used in this work shows the influence of input parameter uncertainties on the output of the developed model. For this, a energy harvesting system subject to periodic excitation was simulated and presented in the following topics.

This work is structured on the following topics: the methodology is presented in section 2, where the reader can find the Mechanical System used and a brief explanation of Sobol' Indices and of Polynomial Chaos Expansion; In section 3 is presented the results of the work and the discussion based on theory of Uncertainty Quantification, a Surrogate Model and Sobol' Indices; In the end, in section 4, is presented the conclusions.

2 Methodology

2.1 Energy Harvesting Mechanical System

A two-degree of freedom physical model for energy harvesting subject to a periodical excitation is shown in

Fig. 1 (Fuzaro de Almeida et al., 2020). This system is composed of two masses (m_1 and m_2), which are interconnected by a spring k_2 and connected to the base by the spring k_1. There are also two dampeners with constant ζ and a piezoelectric transducer v, which converts kinetic energy into electrical energy. The positions of each mass are given by x_1 and x_2, respectively. A periodical excitation is applied at mass m_1 by the action of the force f.

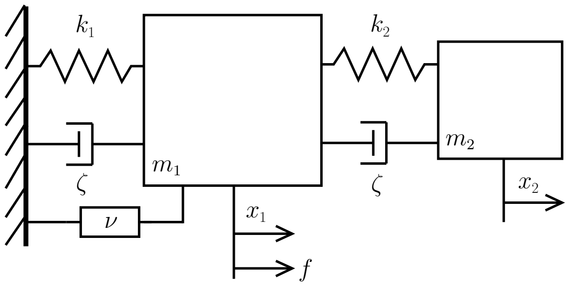

Figure 1: Schematic representation of the energy harvester system studied in the present work.

The system of differential equations which guides the mathematical model is given by Eq. 1. Besides the parameters already shown, there is also χ which is the piezo-electromechanical coupling, Λ is the rate of the reciprocal time constant from the capacitive charging, ω, angular velocity of the periodical excitation, κ, the piezoelectric-electrical coupling and, finally, v is the voltage at the piezoelectric transducer.

$$\begin{cases} \ddot{x}_1 + 2\zeta\dot{x}_1 + k_1 x_1 - k_2\left(x_1 - x_2\right) - \chi v = f\cos\left(\omega t\right) \\ \ddot{x}_2 + 2\zeta\dot{x}_2 - k_2\left(x_1 - x_2\right) = 0 \\ \dot{v} + \Lambda v + \kappa\left(\dot{x}_1 - \dot{x}_2\right) = 0 \end{cases} \tag{1}$$

The main quantity of interest (QoI) associated with the dynamical system under analysis is the mean output power given by

$$\mathcal{P} = \frac{1}{T}\int_{t_0}^{t_0+T} \Lambda v(t)^2 dt \tag{2}$$

which $\mathcal{P}$ is the temporal average of the instantaneous power $\Lambda v(t)^2$ over a given time interval of length T.

2.2 Sobol' Indices

The aim of the present work is to measure the sensibility of the input parameters when a certain randomization is applied to characteristics of the input force (i.e.: amplitude and angular frequency). For this end, a sensitivity analysis based on Sobol method (Sobol, 1990) is applied. The Sobol method or Sobol' indices, gives a total variance measure of a model based on the single or combined variance effects of each of the variable input parameters on a single output quantity of interest (QoI) (Nagel et al., 2020), such as the output electrical power in Eq. 2. This analysis begins by decomposing the (QoI) into summands of different dimensions, as follows:

$$f(X) = f_0 + \sum_i f_i(x_i) + \sum_{i<j} f_{ij}(x_i, x_j) + \cdots + f_{1\cdots n}(x_1, \cdots, x_n) \tag{3}$$

where X is an input vector and $f(X) \equiv f(x_1, x_2, \cdots, x_n)$ is a real-valued function that maps all the inputs into a hypercube with dimensions $K^n \equiv [0,1]^n$ (Rabitz et al., 1999). Each of the function components in 3 are calculated by the following integrals:

$$f_0(x) \equiv \int_{K^n} f(x)dx \tag{4}$$

$$f_i(x_i) \equiv \int_{K^{n-1}} f(x) \prod_{j\neq i} dx_j - f_0 \tag{5}$$

$$f_i(x_i, x_j) \equiv \int_{K^{n-2}} f(x) \prod_{k\notin\{i,j\}} dx_k - f_i(x_i) - f_j(x_j) - f_0 \tag{6}$$

$$f_{i_1\cdots i_l}(x_{i_1}, \cdots, x_{i_l}) \equiv \int_{K^{n-l}} f(x) \prod_{k\notin\{i,\cdots,l\}} dx_k - \sum_{j_1<\cdots<j_{l-1}\subset\{i_1,i_2,\cdots,i_l\}} f_{j_1\cdots j_l}(x_{j_1}, \cdots, x_{j_l}) - \sum_j f_j(x_j) - f_0 \tag{7}$$

given the following null property constrain, for $l = 0, 1, \cdots, n$ and $k = 1, 2, \cdots, l$:

$$f_0(x) \equiv \int_{K^l} f_{i_1\cdots i_l}(x_{i_1}, \cdots, x_{i_l}) dx_{i_k} = 0 \tag{8}$$

it is assured that all the functions are orthogonal,

$$\int_{K^n} f_{i_1\cdots i_s}(x_{i_1}, \cdots, x_{i_s}) f_{j_1\cdots j_p}(x_{j_1}, \cdots, x_{j_p}) dx = 0 \tag{9}$$

when at least one index is different between $\{i_1, ..., i_s\}$ and $\{j_1, ..., j_p\}$, whereas s and p can be equal. Then, taking the variance of both sides of Eq. 3, the total variance of the decomposed function is gotten by the sum over the variances of all its components:

$$D = \sum_{s=1}^{n} \sum_{i_1<\cdots<i_s}^{n} \int f^2_{i_1,\cdots,i_s} dx_i \cdots dx_s \tag{10}$$

Dividing Eq. 10 by D results in what is called "Sobol's indices" or global sensitivity indices (Sobol, 1990). It is worth noting that the following equation is the result of the division of each piece of the summation in 10 and also that, after this division, the sum of all Sobol's indices is equal to unity:

$$S_{i_1,\cdots,i_s} = \frac{D_{i_1,\cdots,i_s}}{D} \tag{11}$$

2.3 Polynomial Chaos Expansion

The usual procedure for evaluating the output of a given model is to use the Monte Carlo method, which basically means repeatedly run the solution of the mathematical model (if known) or an numerical approximation in order to have an estimate of the distribution of the QoI pursued. However, both solutions might induce an overwhelming computational load which could reach the point of being unfeasible. Metamodeling have shown to be a reliable method for coping with said problem (Palar et al., 2018). In the present work, the Polynomial Chaos Expansion (PCE) is the surrogate model technique (metamodeling) that will be implemented. Given an output of a physical model which, in our case, has the format given by Eq. 2, the PCE approximates the output into the following sum (Sudret, 2008):

$$S \approx \sum_{j=0}^{P-1} S_j \Psi_j(X), \quad X = \{x_1, x_2, \cdots, x_n\} \tag{12}$$

where Ψ_j are the Hermite polynomials, orthogonal between themselves, and S_j are unknown coefficients and its amount P is calculated by the following binomial. Eq. 12 is actually the truncated version of the infinite expansion, logically chosen for because of computational purposes and the number of unknown vector coefficients is given by:

$$P = \binom{M+p}{p} \tag{13}$$

for M-dimensional Hermite polynomials of degree not exceeding p. Finally, the metamodeling approximation given by the PCE in Eq. 12 can be directly applied to the calculation of $PC - based$ Sobol' Indices, which is given by:

$$SU_{i_1,\cdots,i_s} = \sum_{\alpha \in A} \frac{S_\alpha^2 E[\Psi_\alpha^2]}{D} \tag{14}$$

where A is the set of tuples that translates into the combination of polynomials that depends only on the parameters $\{x_{i_1}, ..., x_{i_s}\}$. A different notation for this Sobol' indices was given just so it is not misinterpreted as the analytical one (without the metamodeling) given in Eq. 11. The present work will then seek to analyze the effect of random distributions in some of the system parameters over the power output (i.e.: the QoI). For this end, Sobol' Indices will provide a quantitative measure of how much a given value of a parameter influences in the variations of the properties of the model. Furthermore, to reduce the computational cost of the simulations, the surrogate model based on the polynomial chaos expansion will be used.

3 Results and Discussion

For a first investigation of the system's dynamics, numerical experiments were carried out with nominal numerical values for the parameters, i.e., without uncertainties. The nominal values used were: $\chi = 0.05$, $f = 0.2$, $k_1 = 0.09$, $k_2 = 0.02$, $\kappa = 0.5$, $\Lambda = 0.05$, $\omega = 0.8$ and $\zeta = 0.04$. The initial conditions were defined by $[x_1(0); \dot{x}_1(0); x_2(0); \dot{x}_2(0); v(0)] = [0.1; 0; 0.1; 0; 0]$. All of the results provided in this paper were simulated using MATLAB and UQLab modules, and most part of the employed methodology was based on the STONEHENGE repository (Norenberg et al., 2021b).

The system dynamics is obtained by integrating numerically a state space model of Eq. 1 by Dormand-Prince Method (4th order Runge Kutta with variable pitch) over the time interval $0 \leq t \leq 400$ with relative tolerance of 10^{-6}, and absolute tolerance of 10^{-9}. The mean output power is computed over the last 67% of these time-series, in order to remove the transient period.

Subsequently, an analysis was carried out in order to obtain a surrogate model based on PCE that could correctly represent the data obtained by numerical integration via the Dormand-Prince method. This stage is taken to reduce the computing work required in the process of obtaining Sobol indices, which are utilized for sensitivity analysis.

Once the surrogate model was obtained, a global sensitivity analysis was performed. It was assumed that all the system parameters are independent and uniformly distributed over given intervals, which were defined by a coefficient variation (δ) of 20% around the nominal values.

The model was firstly studied by da Costa Ferreira et al. (2016) and complemented over the years by Fuzaro de Almeida et al. (2019, 2020). With the development of a rigorous statistical method, the best modeling of the system so far was reached, investigating which parameters most influences on the mean output power, as described by Eq. 2.

3.1 First step - System dynamics

The first step was to simulate the system using the nominal parameters in order to verify its dynamics, which is sensitive to angular frequency (ω) as shown by Fuzaro de Almeida et al. (2019, 2020). This step is taken to avoid chaotic behavior by not choosing parameters that contributes for the development of this chaotic dynamics, a scenario that is not of interest to this present work. Figs. 2 and 3 show, respectively, the dynamics of the system using the nominal parameters for masses displacement and output voltage, as discussed before.

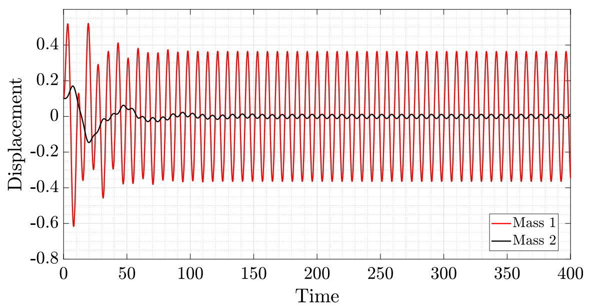

Figure 2: Dynamic behavior of the masses considering nominal parameters.

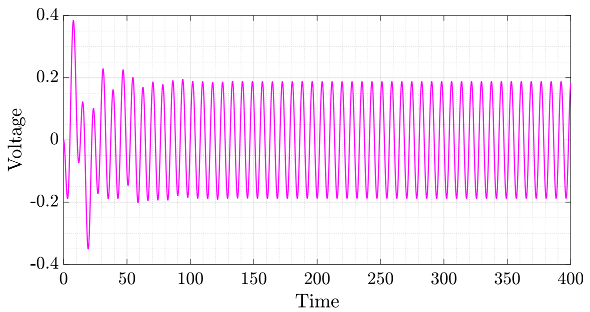

Figure 3: Output voltage in the piezoelectric considering nominal parameters.

It can be seen that for the chosen initial conditions and nominal parameters the system behaves stably and periodically. One thing that is noticeable is the difference between displacement amplitudes of the masses, which is a direct consequence of parameters chosen for the excitation force (ω and f). Finally, it can be concluded that the output voltage has a similar behavior to m_1 due to the coupling effect between them, as presented in Fig. 1.

Next, in order to reduce the computational cost while obtaining the Sobol' indices, a surrogate PCE model was obtained.

3.2 Second step - Surrogate model

In this step, the surrogate PCE model was built using the mean power as a reference. The framework here consists in a comparison between mean power values produced by the full-order model (by directly integrating the numerical model) and the surrogate PCE model (obtained varying sample length and polynomial degree). A reference line was built and it was plotted mean power values of both models: if most part of the points were on the reference line, it could be considered that the surrogate model had a good convergence and accuracy, as shown in the schematic representation of the methodology in Fig. 4. Finally, the accurate PCE model is used to explore several scenarios of parameters variations with low-cost processing, being an advantage when compared with Monte Carlo method, for example.

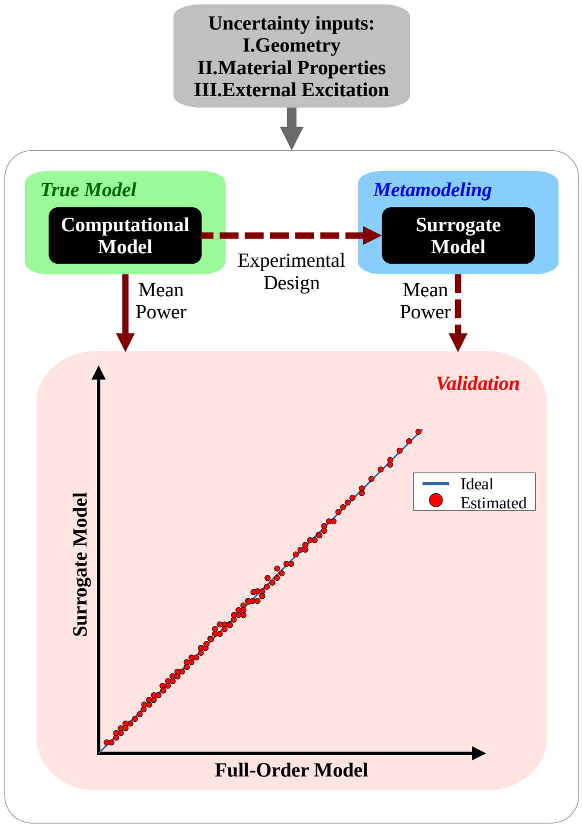

Figure 4: Schematic representation of the methodology utilized to obtain a PCE surrogate model.

Following these steps and using an 8th-degree PCE model with 1000 training samples, it was validated the PCE surrogate model: in Fig. 5 it is possible to correlate the responses $\mathcal{P}_{\text{PCE}}$ of the PCE-based surrogate model and $\mathcal{P}$ of Eq. 2; the closer to the blue line, the more reliable is the PCE-based surrogate model. For this it was used 500 validation samples (x-red-dots).

It can be observed that it was obtained a adequate convergence, validating the surrogate model. The entire time for this simulation was 232 seconds[1] for comparison purposes.

3.3 Third step - Sobol' indices

It was simulated two variations of parameters related to external force: force amplitude (f) and angular frequency (ω). It is desired to investigate how the excitation in general influences on the mean power generation, which is the QoI discussed before on Eq. 2.

[1]Intel i7-9700F 3.00GHz 16GB 2666GHz DDR4 GeForce GTX 1060

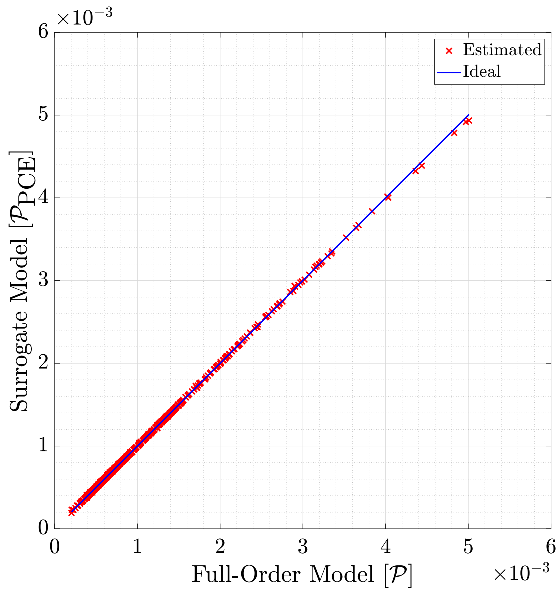

Figure 5: Comparison between $\mathcal{P}_{PCE}$ generated by PCE-based surrogate model and $\mathcal{P}$ from the full-order model.

3.3.1 Force amplitude variation

Firstly, the force amplitude (f) was varied between 0.15 to 0.25 with a step of 0.02. Results are shown in Fig. 6.

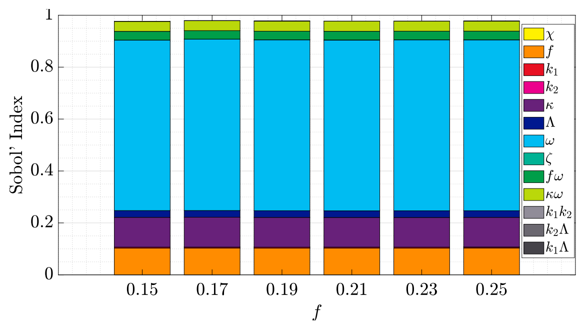

Figure 6: Amplitude force variation Sobol' Indices.

From Fig. 6 it can be seen that ω is the most sensible parameter in the output mean power for all force inputs, representing approximately the same contribution percentage in all cases. In the sequence, κ and f are the second most sensible parameters. And, as the third most sensible parameters, there are some second order Sobol' Indices, which are $f\omega$ and $\kappa\omega$.

In order to evaluate the dynamical behavior of the system, it was plotted two displacement cases: $f = [0.15; 0.25]$. It was just plotted the displacement because the voltage behaves similarly to m_1, which would be redundant. Figs. 7 and 8 present the dynamic behavior of the system for $f = 0.15$ and $f = 0.25$, respectively.

The difference between both dynamics is exclusively in the force amplitude, as expected analyzing

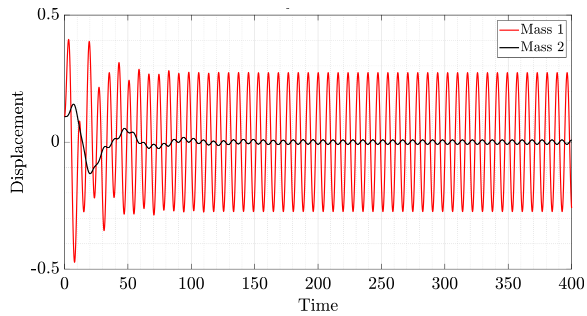

Figure 7: Masses displacement for $f = 0.15$.

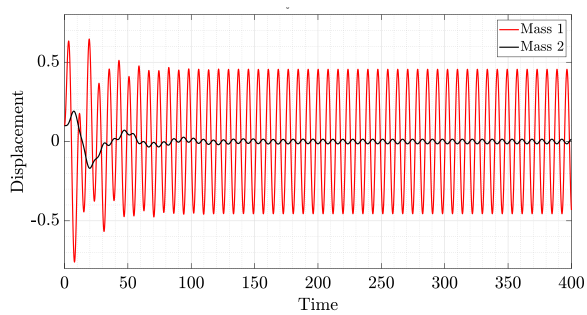

Figure 8: Masses displacement for $f = 0.25$.

Sobol' Indices on Fig. 6. Next, complementing the analysis of how the excitation influences on the mean power generation, it was performed an angular frequency variation.

3.3.2 Angular frequency variation

In complement of the previous results, the angular frequency was varied between 0.1 to 1.0 with a step of 0.05. Results are shown in Fig. 9. And in the Fig. 10 is presented the same results but only the 0.1 to 0.45 interval.

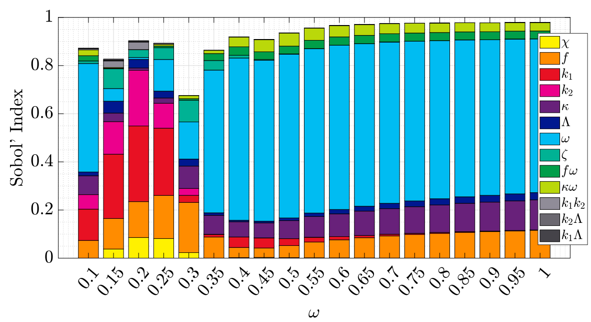

Figure 9: Angular frequency variation Sobol' Indices.

Differing from Fig. 6, it can be noticed from Figs. 9 and 10 that for the interval $0.1 \leq \omega \leq 0.3$ the Sobol' Indices varies a lot. However, even with the variation, it is noticeable that k_1, k_2 and f are the most sensible parameters in the output mean power. The reason will be

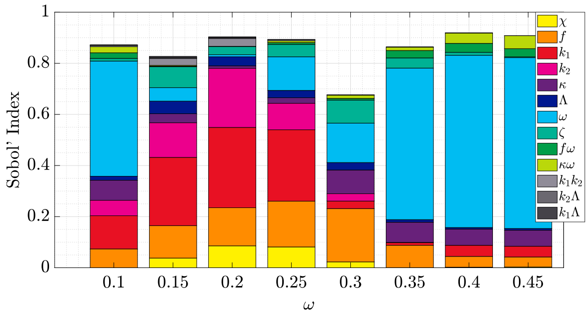

Figure 10: Angular frequency variation Sobol' Indices (zoomed).

clarified analyzing the dynamic behavior of the system.

In the next step, it was evaluated the dynamical behavior of the system, plotting six displacement cases, which are: $\omega = [0.1; 0.2; 0.3; 0.4]$. Figs. 11-14 present the dynamic displacement behavior of the masses for ω values shown in the previous presented sequence (voltage output behavior is similar to m_1, as discussed before).

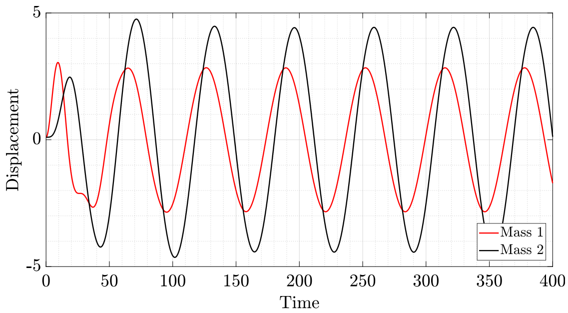

Figure 11: Masses displacement for $\omega = 0.1$.

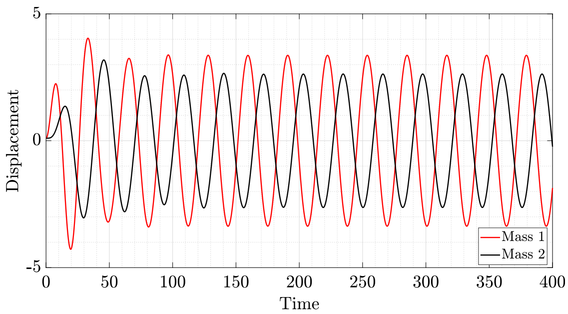

Figure 12: Masses displacement for $\omega = 0.2$.

In a first moment, for Fig. 11, m_1 has a lower, but similar amplitude, and a small phase angle when compared to m_2. When $\omega \geq 0.2$, the amplitude proportion between m_1 and m_2 increases, i.e., m_1 amplitude starts to be greater than m_2's. Another remark is related to the phase angle, that becomes close to π.

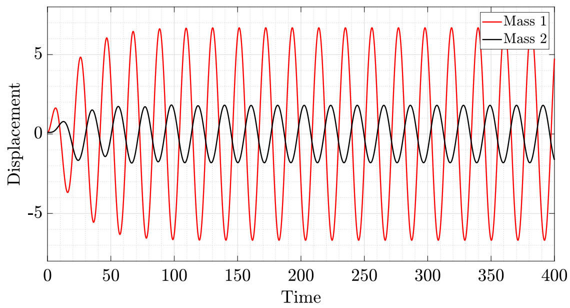

Figure 13: Masses displacement for $\omega = 0.3$.

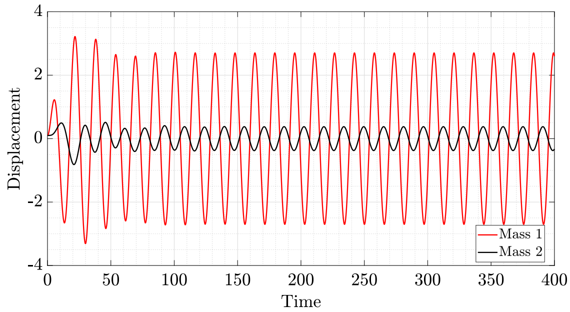

Figure 14: Masses displacement for $\omega = 0.4$.

This phenomenon can be explained by a change on the vibration mode of the system, i.e., a direct consequence of passing by a resonance frequency bandwidth. This explains the greater sensibility of both stiffnesses (k_1 and k_2) in the $0.15 \leq \omega \leq 0.25$ interval, as shown in Fig. 9.

After passing the resonance frequency, the system returns to its regular behavior, i.e., ω being the most sensitive parameter on the mean power generation, followed by κ and f.

In order to investigate how the output mean power behaves with varying ω, an approximation was generated using UQLab's PC-Kriging module (Schöbi et al., 2017).

Polynomial-Chaos-Kriging (PC-Kriging) is a state-of-the-art metamodelling algorithm which was developed by Schöbi et al. (2017) and which is based on the well-established metamodelling techniques Polynomial Chaos Expansions (PCE) and Kriging (Gaussian process modelling)). PC-Kriging makes use of the regression-type PCE to capture the global behavior of the computational model as well as the interpolation-type Kriging to capture local variations. This combination results in a metamodelling technique that is more efficient than PCE and Kriging separately.

Figs. 15 and 16 presents a PC-Kriging approximation using the previous PCE-based surrogate model obtained.

The two natural frequencies of the system become evident as well as the resonance bandwidth. The peak

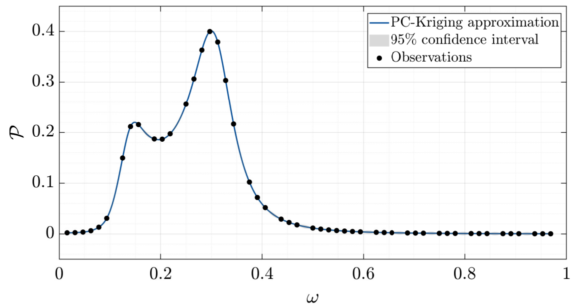

Figure 15: PC-Kriging approximation to investigate the output mean power behavior when varying ω.

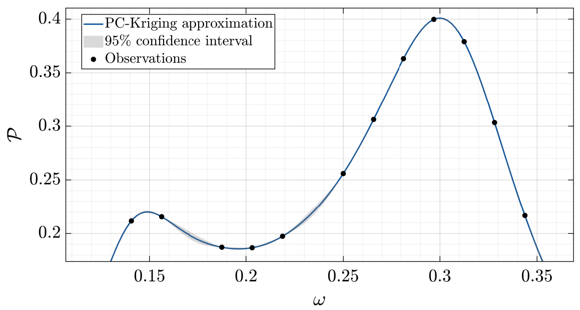

Figure 16: PC-Kriging approximation to investigate the output mean power behavior when varying ω (zoomed).

values in Fig. 16 correspond to the square roots of k_2 and k_1, respectively (since the system is dimensionless by mass). This behavior complements why in Fig. 10 the stiffnesses k_1 and k_2 present the greatest Sobol' Indices: as discussed before, it shows the passing by a resonance bandwith.

4 Conclusions

The Sobol' indices calculation was adequate to determine the sensibility of individual and combined parameters, showing, as well, which of them was the most sensitive parameter affecting the mean power harvested in general; in this case, the angular frequency of the periodical force.

It can be concluded that when the system is excited in a resonance frequency bandwidth, which causes a transition between vibration modes, the most sensitive parameters become the stiffnesses rather than angular frequency. Another matter of interest for metamodeling and simulation was also explored by PCE, it was shown that the method is capable of represent with optimal fidelity the behavior of an energy harvesting system using little computational effort, which is a big problem in modern computational simulations.

A multimodal energy harvester was studied, whose the main characteristic is to provide a larger resonance bandwidth, improving the energy harvesting efficiency in a wider range of possibilities. The results obtained in this work reveal the need in quantifying and propagating uncertainties in multimodal energy harvesting systems, considering their capacity of harvest energy from sources that, nowadays, are considered dissipated/lost energy. Furthermore, the framework proposes a powerful tool to develop a robust design, to forecast, and to optimize multimodal energy harvesting systems.

4.1 Roadmap of future works

The next step is to evaluate the same system operating with a non-ideal excitation source, complementing the work of Fuzaro de Almeida et al. (2020).

Acknowledgements

The authors would also like to thank the financial support of the following Brazilian agencies: Coordination for the Improvement of Higher Education Personnel (CAPES) - Grant No. 88887.639569/2021-00; São Paulo Research Foundation (FAPESP) - Grants No. 2017/03829-7, 2018/26690-7 and 2021/06133-9; and National Council for Scientific and Technological Development (CNPq) - Grant No. 129972/2021-5.

The authors would also like to thank Prof. Américo Cunha Junior for teaching the course on Uncertainty Quantification, which is part of the Graduate Program in Mechanical Engineering at the Ilha Solteira School of Engineering. The course, as well as the knowledge transmitted, were the great motivators for this work to be developed. In parallel the authors would like to thank João Pedro Noremberg for presenting the methodology used in this work as well as the disposability of the STONEHENGE repository (Norenberg et al., 2021b).

Authors' contributions

Estênio and João planned the scheme, initiated the project, and suggested the experiments; Estevão and Estênio conducted the experiments and analyzed the empirical results; Estevão and Lucas developed the mathematical modeling and examined the theory validation. The manuscript was written through the contribution of all authors. All authors discussed the results, reviewed, and approved the final version of the manuscript.

Code availability

The simulations reported in this paper used the computational code available for free in GitHub directory named and available as: inSANE_HAPEX.

Conflict of interest

The authors declare that they have no known competing financial interests or personal relationships that could have appeared to influence the work reported in this paper

References

Fuzaro de Almeida, Estevão, Fabio Roberto Chavarette, and Douglas da Costa Ferreira. 2019. Optimal linear control applied in a energy harvesting dynamic system with periodic excitation. In *Proceedings of the 25th International Congress of Mechanical Engineering*. ABCM.

Fuzaro de Almeida, Estevão, Fábio Roberto Chavarette, and Douglas da Costa Ferreira. 2020. Potência gerada em um sistema dinâmico de captação de energia controlado via método lqr: Comparação entre excitação periódica e não-ideal. In *Colloquium Exactarum. ISSN: 2178-8332*, volume 12, pages 62–76.

da Costa Ferreira, Douglas. 2015. *Projeto de controladores para a maximização de sistemas de captação de energia considerando excitação não ideal.* Ph.D. thesis, São Paulo State University.

da Costa Ferreira, Douglas, Fábio Roberto Chavarette, Luiz Ricardo de Almeida, Renato Santos de Souza, and Luis Paulo Morais Lima. 2016. Multimodal energy harvesting efficiency enhancement via linear matrix inequalities control driven. *Proceeding Series of the Brazilian Society of Computational and Applied Mathematics*, 4(1).

Massone A. C. C., Viola F. M., de Oliveira Reis S. 2019. Vibration energy harvesting using piezoelectric materials. *Conhecimento & Diversidade*, 11(25):63–80.

Nagel, Joseph B., Jörg Rieckermann, and Bruno Sudret. 2020. Principal component analysis and sparse polynomial chaos expansions for global sensitivity analysis and model calibration: Application to urban drainage simulation. 195:106737.

Norenberg, João Pedro, Americo Cunha Jr, Samuel da Silva, and Paulo Sérgio Varoto. 2021a. Global sensitivity analysis of (a) symmetric energy harvesters. *arXiv preprint arXiv:2107.04647*.

Norenberg, João Pedro, João Victor Peterson, Vinicius GonçalvesLopes, Roberto Luo, Leonardo de la Roca, Marcelo Pereira, José Geraldo Telles Ribeiro, and Americo Cunha Jr. 2021b. Stonehenge—suite for nonlinear analysis of energy harvesting systems. *Software Impacts*, page 100161.

Palar, Pramudita Satria, Lavi Rizki Zuhal, Koji Shimoyama, and Takeshi Tsuchiya. 2018. Global sensitivity analysis via multi-fidelity polynomial chaos expansion. *Reliability Engineering & System Safety*, 170:175–190.

Rabitz, Herschel, Ömer F. Aliş, Jeffrey Shorter, and Kyurhee Shim. 1999. Efficient input—output model representations. 117(1-2):11–20.

Schöbi, R, S Marelli, and B Sudret. 2017. Uqlab user manual–pc-kriging. *Report UQLab-V1*, pages 1–109.

Sobol, Il'ya Meerovich. 1990. On sensitivity estimation for nonlinear mathematical models. *Matematicheskoe modelirovanie*, 2(1):112–118.

Sudret, Bruno. 2008. Global sensitivity analysis using polynomial chaos expansions. *Reliability Engineering & System Safety*, 93(7):964–979.